Title
Methodology to Characterize the Seismic Compression of Unsaturated Sands under Different Drainage Conditions

Journal
Geotechnical Testing Journal, 44(2)

ISSN
0149-6115

Authors
Rong, Wenyong
McCartney, John Scott

Publication Date
2021-03-01

DOI
10.1520/gtj20190340

Peer reviewed

METHODOLOGY TO CHARACTERIZE THE SEISMIC COMPRESSION OF UNSATURATED SANDS UNDER DIFFERENT DRAINAGE CONDITIONS

By W. Rong, S.M.ASCE[1] and J.S. McCartney, Ph.D., P.E., F.ASCE[2]

ABSTRACT: This study focuses on a new experimental setup and methodology to characterize the volumetric contraction of unsaturated sands during cyclic shearing under different drainage conditions. A new cyclic simple shear device was developed with suction-saturation control using a hanging column suitable for testing unsaturated granular soils with a maximum suction of 11 kPa. The pore water and pore air pressures are monitored during cyclic shearing using an embedded tensiometer and a gauge pressure transducer protected by a hydrophobic filter, respectively. In addition to describing the specimen preparation techniques and testing methodology, typical results for the seismic compression of nearly-saturated, dry, and unsaturated sand specimens during cyclic shearing under different drainage conditions are compared. The differences in the response of these sand specimens were interpreted using the changes in mean effective stress and secant shear modulus during cyclic shearing. The unsaturated sand specimen showed lower seismic compressions than the dry sand specimen and the nearly-saturated sand specimen in drained conditions. A greater contraction observed for the unsaturated sand specimen in undrained conditions was attributed to decreases in mean effective stress and secant shear modulus associated with a decrease in matric suction due to different rates of pore water and air pressure generations and an increase in degree of saturation due to volumetric contraction.

KEYWORDS: Cyclic simple shear; Unsaturated soils; Seismic compression

[1] Graduate Research Assistant, Department of Structural Engineering, University of California San Diego, 9500 Gilman Dr. La Jolla, CA 92093-0085; Email: w1rong@eng.ucsd.edu

[2] Professor and Department Chair (Corresponding Author), Department of Structural Engineering, University of California San Diego, 9500 Gilman Dr. La Jolla, CA 92093-0085; Email: mccartney@ucsd.edu

INTRODUCTION

Unsaturated soils are often encountered in engineered geostructures like embankments or retaining walls involving compacted backfills, in near-surface natural soil layers above the water table, and even in natural soil deposits below the ground water table where occluded air bubbles are present due to ground water level fluctuations or decomposition of organic materials (Tsukamoto et al. 2002). Although one of the greatest potential impacts of earthquakes on soil layers is liquefaction and the associated loss in shear strength, the liquefaction resistance of soils increases remarkably with even a small reduction in the degree of saturation (Chaney 1978; Yoshimi et al. 1989; Ishihara 2001; Tsukamoto et al. 2002; Mele et al. 2019). Okamura and Soga (2006) suggested two possible mechanisms that contribute to the enhancement of the liquefaction resistance of unsaturated soils. The first mechanism is the existence of pore air in the form of the occluded air bubbles that could absorb excess pore water pressure during undrained cyclic shearing by reducing its volume. The second mechanism is associated with the increased interparticle connections due to the impacts of matric suction and degree of saturation on the stress state. While several studies found that unsaturated soils can liquefy under some conditions (i.e., certain combinations of cyclic shear strain magnitude and number of cycles), these conditions are more severe than those causing liquefaction of saturated soils (Yoshimi et al. 1989; Unno et al. 2008; Kimoto et al. 2011; Mele et al. 2019). While liquefaction of unsaturated soils having relatively high initial degrees of saturation (above 70%) may be an important failure mechanism to consider in seismic analyses, seismic compression may become more relevant for unsaturated soils with lower degrees of saturation (Whang et al. 2000; Stewart et al. 2001; Stewart et al. 2004; Rong and McCartney 2019, 2020a, 2020b, 2020c). In engineered soil layers, even small seismically-induced settlements may have a major effect on overlying structures like bridge decks, roadways, or railways. Although empirical formulations are available for estimating seismic compression of unsaturated sand layers under different earthquake shaking events (e.g., Yee et al. 2011; Ghayoomi et al. 2013), some of the relationships in these formulations do not consider the hydro-mechanical coupling that may occur during cyclic shearing.

Seismic compression of unsaturated soils is a complex problem as it may occur in both drained (slow cyclic shearing) and undrained conditions (faster cyclic shearing). Volume changes may be resisted by interparticle stresses which could change with shear-induced excess pore water pressures. Volumetric contraction also leads to increases in the degree of saturation. Coupled changes in pore air pressure, pore water pressure, and degree of saturation, together with volume change effects on the soil-water retention curve (SWRC) of soils, will lead to complex changes in the effective stress (Bishop and Blight 1963; Lu et al. 2010). Further, the effective stress is closely linked with the shear modulus and damping at both small and large cyclic shear strains (Khosravi et al. 2010; Hoyos et al. 2015; Le and Ghayoomi 2017; Dong et al. 2016, 2017). To evaluate the seismic compression of unsaturated sands in an experiment, careful monitoring of the volume, pore water pressure, pore air pressure, and volumetric outflow (for drained conditions) is needed during cyclic shearing. This information can be used to interpret the state parameters like the degree of saturation and matric suction as well as the SWRC and effective stress.

To address the challenges in measuring the seismic compression of unsaturated sands, a new cyclic simple shear device was developed that includes a hanging column for suction-saturation control along with special top and bottom caps that permit independent measurements of pore water pressure and pore air pressure, respectively, during cyclic shearing under different drainage conditions. The capabilities of this device were investigated through drained and undrained cyclic shearing tests on sand specimens with an initial relative density of 0.45 in dry, nearly-saturated and unsaturated conditions. The unsaturated sand specimens evaluated in this study have relatively low initial degree of saturation (0.3) that fall in the funicular regime of the SWRC (Lu and Likos 2004). The reasons for focusing on an initial degree of saturation in the funicular regime are that the chances of liquefaction are relatively low but the coupling between the pore fluid pressures, degree of saturation, volume change, and effective stress is expected to be high.

BACKGROUND

Simple Shear Device

Monotonic simple shear testing was originally developed to measure the stress-strain and in-situ shear strength of highly sensitive clays encountered in disastrous slope failures in Norway (Bjerrum and Landva 1966). Monotonic simple shear testing permitted evaluation of soil behavior under stress paths that were closer to those responsible for triggering slope failures than those achieved in triaxial testing. Since that time cyclic simple shear testing has been used extensively to measure the dynamic properties of soils (i.e., the shear modulus and damping ratio) as a function of cyclic simple shear strength (Hardin and Drnevich 1972; Doroudian and Vucetic 1995; Vucetic et al. 1998), along with the shear-induced volume change behavior associated with void collapse in dry soils (Seed and Idriss 1971; Finn et al. 1976; Dobry and Petrakis 1990) and liquefaction in water-saturated soils (Ishihara et al. 1975; Martin et al. 1975; Ishihara and Yoshimine 1992), as it allows free rotation of principal stresses within the soils in a cyclic manner and it is thus considered more suitable for the simulation of the stress-strain behavior of soils expected during earthquakes.

Recent experimental advancements have extended the potential of the simple shear apparatus to unsaturated soils to address the increasing demands in engineering profession for understanding the unsaturated effect on the dynamic properties of soils and the mechanism governing the volume change in monotonic and cyclic loading conditions. Most modifications for monotonic loading conditions were aimed at understanding the triggering mechanisms of rainfall-induced landslides involving unsaturated soils and special attention has been given to the volume change of unsaturated soils on wetting (Sorbino et al. 2011; Cuomo et al. 2017). Most previous studies focused on the cyclic shearing of unsaturated soils used cyclic triaxial devices (Okamura and Soga 2006; Unno et al. 2008; Okamura and Noguchi 2009; Craciun and Lo 2009; Oka et al. 2010; Kimoto et al. 2011; Zhou and Ng 2016). An issue with cyclic triaxial testing is that the use of a one-sided loading path involving compression only without a stress-strain reversal (e.g., Zhou and Ng 2016), or a loading path that does provide a symmetric stress-strain reversal, (e.g., Unno et al. 2008 and Mele et al. 2019) may affect the generation of pore air and water pressures.

Fewer studies have focused on the cyclic shearing on unsaturated soils using cyclic simple shear devices despite their advantage in applying full reversals of shear similar to that observed in earthquakes. Early studies using cyclic simple shear devices investigated unsaturated soils without control of the suction or measurement of changes in degree of saturation during shearing (Whang et al. 2004, 2005; Duku et al. 2008), so the role of unsaturated conditions was not fully understood. Rahnenma et al. (2003) implemented the axis translation technique to control and measure matric suction within a cylindrical simple shear device that can perform both monotonic and cyclic shearing tests. Milatz and Grabe (2015) used a computer controlled vacuum regulator to apply negative water pressures to the base of a stacked-ring type simple shear device, and water outflow was measured using a horizontal pipette. A flexible membrane was incorporated inside the stacked ring device to prevent leakage of fluids. They also used an embedded tensiometer to measure changes in pore water pressure during cyclic shearing. Although their suction-saturation control approach is similar to the hanging column approach used in this study, they did not include an approach to independently measure changes in pore air pressure. Instead the top cap of the specimen was vented to atmosphere, and the cyclic shearing tests were partially drained (drained air but undrained water). Le and Ghayoomi (2017) modified a stacked-ring type cyclic simple shear apparatus to investigate the strain-dependent dynamic properties of unsaturated sand, which used the axis translation technique and a tensiometer to control and measure the matric suction, respectively. However, their study focused on the dynamic properties of unsaturated sands in drained condition at the first few cycles and no special attention has been given to the hydro-mechanical coupling during cycles of shearing. Le and Ghayoomi (2017) also did not include an approach to measure changes in pore air pressure during undrained cyclic shearing, but different than Milatz and Grabe (2015) they performed fully drained tests (drained air and drained water).

The authors have applied the experimental setup and methodology described in this paper to investigate the trends in the seismic compression of unsaturated sands having different initial degrees of saturation in the funicular regime. Rong and McCartney (2020a) interpreted drained seismic compression results presented by Rong and McCartney (2019) to understand the evolution in effective stress associated with the increasing degree of saturation during volumetric contraction and to develop a model for predicting the drained seismic compression after many cycles of shearing. Rong and McCartney (2020b) interpreted undrained seismic compression data from Rong and McCartney (2020c) to understand the independent evolution in hydro-mechanical variables for unsaturated sand specimens in the funicular regime and discovered that all specimens followed the same trend between volume change and effective stress. This paper describes the methodology and setup used in these other studies that were focused on understanding specific issues, and includes more detailed interpretation for dry, nearly-saturated, and unsaturated sand specimens to demonstrate the approach. It also includes a comparison between the results from this approach with others described in this literature review.

Effective Stress in Unsaturated Soils

Many mechanical properties of soils, including the shear strength, shear modulus, and damping ratio, are directly related to the effective stress. To extend the mechanistic framework established for saturated soils to unsaturated soils, Bishop (1959) proposed the following definition of effective normal stress for unsaturated soils:

$$\sigma' = (\sigma - u_a) + \chi(u_a - u_w) \quad (1)$$

where σ is the total normal stress, u_a is the pore air pressure, u_w is the pore water pressure, and χ is Bishop's effective stress parameter. The difference between total normal stress and air pressure is referred to as the net normal stress and the difference between pore air and pore water pressures is referred to as the matric suction. Many definitions of the effective stress parameter χ have been proposed in the literature, some related to the suction and others related to the degree of saturation. Lu et al. (2010) replaced the product of χ and matric suction in Equation 1 with a single term called suction stress σ_s that incorporates all interparticle forces. They calculated suction stress by assuming χ is equal to the effective saturation S_e, which can be defined as follows:

$$S_e = \frac{S - S_{res}}{1 - S_{res}} \quad (2)$$

where S is the degree of saturation and S_{res} is the residual saturation. This assumption for χ has the advantage that the SWRC can be integrated into the definition of effective stress. The effective saturation can be related to suction through the van Genuchten (1980) SWRC model, as follows:

$$S_e = \left\{\frac{1}{1 + [\alpha_{vG}\,(u_a - u_w)]^{N_{vG}}}\right\}^{1-\frac{1}{N_{vG}}} \quad (3)$$

where a_{vG} and N_{vG} are the van Genuchten (1980) SWRC fitting parameters. The effective stress definition of Lu et al. (2010) obtained by combining Equations (1) and (3) is given as follows:

$$\sigma' = (\sigma - u_a) + \left[\frac{u_a - u_w}{\left(1 + [\alpha_{vg}(u_a - u_w)]^{N_{vg}}\right)^{1 - \frac{1}{N_{vg}}}}\right] \tag{4}$$

In this equation, the term in brackets can be referred to as the suction stress σ_s, and the relationship between suction stress and matric suction (or degree of saturation) is referred to as the suction stress characteristic curve (SSCC). In this study, Equation (4) will be used to quantify the stress state of unsaturated soils. Khosravi and McCartney (2009) synthesized test results from several studies on unsaturated soils and found that the relationship between small-strain shear modulus and effective stress follows a similar power law relationship to that commonly used for saturated and dry soils. However, Khosravi et al. (2010) found that using a suction stress equal to the matric suction (i.e., χ=1) led to a good fit in matching the trend in measured small-strain shear modulus of clean sand with effective stress. Dong et al. (2016) found that a relationship between effective stress and small strain shear modulus that incorporates the degree of saturation provides a good fit for many types of soils including sands.

CYCLIC SIMPLE SHEAR APPARATUS WITH SUCTION-SATURATION CONTROL

Cyclic Shearing Mechanism

Characterization of the seismic compression of unsaturated sands requires special considerations to monitor the pore water and the pore air, as well as the capability to control the unsaturated states of soils. In this study, a monotonic simple shear apparatus manufactured by the Norwegian Geotechnical Institute (NGI) was modified to perform cyclic tests on unsaturated sands incorporating a hanging column setup to control the matric suction and monitor outflow needed to evaluate changes in degrees of saturation. A picture of the new simple shear apparatus is shown in Figure 1. The horizontal forces are applied using a linear actuator (ETH series manufactured by Parker) driven by a brushless rotary motor with low backlash (BE series manufactured by Parker).

The system was configured to apply displacement-controlled cyclic motions with smooth transitions during reversals in movement. The stroke range of the linear actuator is 50 mm and the motor can apply a maximum continuous torque of 4.8 N-m at a maximum speed of 0.33 m/s. The motor system is controlled using a drive module (SPiiPlus CMnt module by ACS Motion Control) connected to a rotary encoder on the motor. A rigid transmission frame was designed to transmit horizontal forces from the motor to the top cap of the specimen to eliminate tilting. Vertically oriented bearings on either side of the transmission frame also permit free vertical displacement of the top cap in response to volume changes of the soil specimen.

Instrumentation

A high-accuracy S-Beam tension and compression load cell with a capacity of 2224 N (model LSB350 manufactured by Futek of Irvine, CA) was installed between the rigid transmission frame and the linear actuator to measure the horizontal force during displacement-controlled cyclic shearing. Two DC voltage output linear displacement transducers (model LD620 manufactured by Omega Engineering of Norwalk, CT) with a stroke range of 5 mm and a resolution of 0.001 mm were used to measure the cyclic shear displacement and the vertical settlement experienced in the soil specimen. A tensiometer (model T5 obtained from UMS GmbH of Munich, Germany) with a range of -85 kPa to 100 kPa and a resolution of 0.01 kPa was used to monitor pore water pressures in the soil specimen. The tensiometer was used to both verify the pore water pressure applied to the specimen using the hanging column approach and to measure changes in pore water pressure during undrained shearing. The tensiometer has a small ceramic tip with a surface area of 50 mm^2 and a slender shaft filled with a small amount of de-aired water, which exerts negligible impact on the soil specimen during test while measuring, but was found to provide a sufficiently fast response time for the rates of shearing applied in this study, as demonstrated in the results. Additionally, to measure the pore air pressure separately in fully undrained tests, a gauge pressure transducer (model PXM409 manufactured by Omega Engineering of Norwalk, CT) with a measurement range of 0 to 100 kPa and a resolution of 0.01 kPa was utilized. The linear displacement transducers were monitored using a NI 9219 data acquisition module while the load cell, tensiometer, and gauge pressure sensor were monitored using a NI 9237 data acquisition module. Both data acquisition modules are manufactured by National Instruments of Austin, TX.

Hanging Column Device for Suction-Saturation Control

To control the initial conditions of soil specimens and to assess the effect of pore water and pore air during testing in different drainage conditions, a special specimen housing with separate routes for the measurements of pore water and pore air was designed for the cyclic simple shear device. A schematic of the specimen housing and the hanging column is shown in Figure 2. The cylindrical specimen has a height of 20 mm and a diameter of 66.7 mm, resulting in a height to diameter ratio of H/D = 0.3, which is less than the maximum value of 0.4 set by ASTM D6528-17, *Standard Test Method for Consolidated Undrained Direct Simple Shear Testing of Fine Grain Soils*. The hanging column shown in this schematic was developed based on the approach used by Khosravi et al. (2010) that uses a graduated Marriotte burette to monitor inflow and outflow of water while maintaining a constant head.

Lateral confinement of the specimen was maintained using a wire-reinforced rubber membrane (diameter 66.8 mm, manufactured by Geonor), shown in Figure 3(a). This membrane provides lateral constraint and minimizes radial deformation of the specimen during preparation, application of vertical stresses, and cyclic shearing but allows vertical and shear deformation with negligible stiffness from the boundaries. Therefore, K_0 conditions can be assumed when quantifying the mean effective stress of the unsaturated specimens during cyclic simple shear testing.

The top platen incorporates a coarse porous stone and recessed grooves for air drainage or pore air pressure measurements in undrained condition while providing a rough surface to transmit shear stresses to the top boundary of the specimen. To increase friction between the specimen and the top cap and to ensure horizontal displacement fully applied to the top of the specimen during cyclic shearing, the top cap of the specimen housing, shown in Figure 3(b), is specially designed with several embedded vertical pins that intrude approximately 2 mm into the top of the specimen. Prior to pushing the pins into the top of the soil specimen, the pins are pushed through a hydrophobic filter which helps minimize the movement of pore water into the top cap while allowing free passage of pore air. This hydrophobic membrane was found to improve the measurement of the pore air pressure during undrained shearing. It is also assumed that during cyclic shearing, where the top platen is moved horizontally with respect to the bottom platen, the shear stress is equally distributed on the horizontal cross section of the specimen. The bottom platen incorporates a circular fritted glass disk with an air-entry suction of 50 kPa that transmits water from a hanging column consistent with ASTM D6836 but cut off the flow of air so that pore water pressure can be measured. The edge of the fritted glass disk would be sealed with epoxy to prevent leakage so that pore air and pore water can be accurately controlled. The fritted glass disk has a drilled channel in the center to permit insertion of the tensiometer through the base platen into the lower portion of the soil specimen to monitor changes in pore water pressure during cyclic shearing, shown in Figure 3(c). The tensiometer can be used to monitor the pore water pressure during initial suction application as well as during either drained or undrained shearing. An insertion distance of 3 mm from the base (15% of the specimen thickness) is expected to be sufficient to measure shear-induced pore water pressures without having major effect on the formation of shearing planes in the specimen. An “O”-ring, as well as silicon sealant, was used before the preparation of specimens to seal the small gap between the fritted glass disk and the tensiometer tip to prevent leakage of pore air and pore air during testing. The hydraulic seal provided by this approach prevented leakage of fluids around the fritted glass disk but could be readily removed and replaced.

Before the application of negative water pressures to the specimen to reach the target degree of saturation or matric suction, the flushing port at the bottom was kept open so that any trapped air bubbles below the fritted glass disk can be flushed out prior to the application of negative water pressures, shown in Figure 3(d). The flushing port was then closed if no air bubbles were observed to flush out, and negative water pressure is applied to the bottom of the saturated fritted glass plate by changing the elevation of the hanging column with respect to the base of the specimen while the air path in the top platen is kept open ($u_a = 0$ in the specimen). The matric suction, which is the absolute value of the applied negative water pressure when $u_a = 0$, will vary with height in the specimen due to the elevation head, but for 20 mm-thick specimens, the suction difference between the top and bottom of the specimen will be 0.2 kPa and the suction can be assumed to be uniform. Based on the height of the benchtop used to support the simple shear device, the hanging column used in this study can apply negative water pressures up to 11 kPa, which is sufficient to reach the funicular region of the SWRC of most sands (McCartney and Parks 2009). As mentioned, the hanging column system can track outflow from the specimen during drained cyclic shearing tests while maintaining a constant head using a specialized Mariotte tube built from a graduated burette, similar to that used by Khosravi et al. (2010). If water flows out of the Mariotte tube (i.e., during imbibition of the specimen), a vacuum will naturally occur within the burette which will cause bubbling to occur, making the pressure head at the tip of the bubbling tube equal to zero. However, if water flows into the Mariotte tube (i.e., during specimen drainage), then an external vacuum must be applied to the top of the burette with a magnitude equal to the pressure exerted by the height of water H. This external vacuum is controlled using a regulator, with a magnitude selected manually to maintain steady bubbling in the burette.

MATERIAL PROPERTIES

The sand used in this study is classified as a well-graded sand (SW) according to the Unified Soil Classification System (USCS) and was previously used in the shaking table experiments on mechanically-stability earth bridge abutments performed by Zheng et al. (2018). The particle size distribution curve of the sand is shown in Figure 4, and the mean grain size D_{50} and the effective grain size D_{10} are 0.8 mm and 0.2 mm, respectively. The sand has a coefficient of uniformity of C_u = 6.1 and a coefficient of curvature of C_c = 1.0. The specific gravity is 2.61, and the maximum and minimum void ratios are 0.853 and 0.371, respectively. The SWRC of the sand at a relative density of 0.45 was measured using a different hanging column setup that can apply higher suction magnitudes than the cyclic simple shear device.

To measure the SWRC, a pre-determined mass of dry sand was poured at a constant rate from a funnel into a Büchner funnel having a fritted glass disk with an air-entry suction of 50 kPa at the bottom that was filled with de-aired water. It was found that a target density of 0.45 could be reached reliably without tamping. This specimen preparation approach is similar in principle to that adopted by Tatsuoka et al. (1979). This initially saturated specimen was incrementally desaturated by applying negative water pressures (u_w) to the hanging column while leaving the surface of the specimen open to the atmosphere (air pressure u_a = 0). Once the outflow of water from the bottom boundary remained constant over a time between readings of 30 minutes, the sand specimen was assumed to be at hydraulic equilibrium. Different regimes of the SWRC defined by Lu and Likos (2004) are shown in Figure 5(a), along with the test results including the primary drying path and the primary wetting path: the capillary regime where soils remain saturated under negative pore water pressure, the funicular regime where the water phase is continuous, and the residual regime where the water phase is discontinuous. The best-fit SWRC model parameters are summarized in Table 1. The air-entry suction ψ_{aes} of the sand at the relative density of 0.45 was found to be 1.43 kPa using the graphical approach proposed by Pasha et al. (2015), shown in Figure 5(b), which considers volume change of the specimen during desaturation. The best-fit values of the parameters a_{vG} and N_{vG} for the drying path were used to define the SSCC, which is plotted in terms of both degree of saturation and matric suction in Figure 6. Lu et al. (2010) found that if the value of N_{vG} is greater than 2.0, as is the case for the sand tested in this study, the SSCC does not increase monotonically with suction but instead increases with suction (or decreasing degree of saturation) up to a certain value (1.15 kPa for this sand) then decreases to zero at high suctions.

SPECIMEN PREPARATION

Unlike the wet tamping method used in previous studies on seismic compression involving unsaturated soils (e.g., Whang et al. 2004, 2005; Duku et al. 2008), which may lead to different soil structures, the initial unsaturated conditions of sand specimens were achieved by desaturation on the saturated specimens in this study. The bottom platen of the specimen housing was first fastened on the simple shear device using the T-clamps, and the tensiometer was inserted through the porous glass disk and sealed with an "O"-ring into place to prevent leakage. To avoid preferential flow of air around the edges of the fritted glass disk, epoxy was used to seal to the base platen around the outer edges and the space around the tensiometer was sealed using silicone prior to the preparation of sand specimens, as shown in Figure 3(c). Several pore volumes of de-aired pore water were passed upward through the fritted glass disk to ensure saturation of the disk. A wire-reinforced rubber membrane was installed and fastened to the bottom platen using a pair of "O"-rings. Dry pluviation was used to place pre-weighed sand into the space within the membrane through a funnel with a low drop height to reach a target relative density of 0.45. The water level in the initially dry sand specimen was then slowly raised by maintaining the water level in the graduated burette higher than the top of the sand specimen. The sand specimen was assumed nearly-saturated if de-aired water was observed to leave the top of the specimen. S was found to reach as high as 0.94 for the initially dry sand used in this study without the application of backpressure when following this approach. After leveling the top of the sand specimen, the top cap with the hydrophobic filter paper was placed on the top of the specimen and the wire-reinforced rubber membrane was fastened to the top cap with a pair of "O"-rings. Finally, a vertical stress was applied to the top of the sand specimen using dead weights and the top cap was fastened to the shearing plate of the cyclic simple shear device.

To prepare the unsaturated specimens, saturated specimens were desaturated using the hanging column to reach the target matric suction. Water outflow was monitored during the process, and the tensiometer reading was used to confirm that the target matric suction was reached. Once the reading of the tensiometer was constant and the water outflow did not change over 30 minutes, the unsaturated specimen is assumed to be at hydraulic equilibrium and ready for shearing.

TESTING PROCEDURES

Prior to cyclic shearing, the top cap was fastened to the rigid shearing plate on the simple shear device and the actual initial height of the unsaturated specimen under the applied vertical stress was measured so that volumetric strains during cyclic shearing can be calculated from the change in height. In the drained constant suction test, the gauge air pressure transducer was not connected and the grooved air path in the top platen was left open. Thus, the pore air pressure within the specimen was atmospheric during the drained experiments, and the matric suction was equal to the negative of the applied negative water pressure (i.e., a positive value) at the bottom of the specimen housing. Water outflow from the sand specimen, due to the volumetric contraction during cyclic shearing, was collected and measured using the graduated burette while the vacuum regulator was operated carefully to ensure a steady flow of air bubbles in the graduated burette so that constant suction can be maintained in the drained test. In the fully undrained constant water content test, the gauge air pressure transducer was firmly connected to the sealed fitting on the top platen so that excess pore air pressure can be measured separately. The amount of the space between the air pressure transducer and the top boundary of the specimen is small enough to ensure the accurate measurement of the pore air pressure in the unsaturated sand specimen. And the drainage valve for the water at the bottom was closed so that pore water pressure can be measured through the inserted tensiometer. Pore water and pore air are expected to be pressurized due to the volume contraction during undrained cyclic shearing. Further, the volume of the unsaturated sand specimen is expected to change during both drained and undrained cyclic shearing due to the compression of the pore air.

EXPERIMENTAL RESULTS AND DISCUSSION

Testing Program Overview

In this study, strain-controlled cyclic shearing tests on dry, nearly-saturated, and unsaturated specimens in both drained and undrained conditions were performed to validate the capability of the cyclic simple shear apparatus with suction control system to characterize seismic compression of unsaturated sands. The selected three initial conditions are shown on the SWRCs in Figure 5(a) as well. Nearly-saturated and dry conditions cannot be plotted on a logarithmic scale for matric suction but are still shown on the plot as points A and C, respectively. Based on the SWRC fit in Figure 5(a), the dry specimen (θ_w = 0) is assumed to have a matric suction of 100 kPa. Although the sand specimen cannot be fully saturated without the application of cell pressures in the current setup, the nearly-saturated sand specimen having a zero matric suction is assumed equivalently as saturated for the purpose of characterizing seismic compressions in this study, as the volume of pore air in the nearly-saturated state is small and its effect on the volume change of the sand specimen during cyclic shearing under the stress condition evaluated in this study is negligible.

Although the test device is capable of applying cyclic shear strains with different amplitudes, along with sufficient accuracy, a representative cyclic strain γ_c of 1% was applied with the same number of cycles N = 200 for all the specimens in this study, as shown in Figure 7. The goal of choosing this number of cycles was to allow the hydro-mechanical processes to stabilize to demonstrate the capabilities of the cyclic simple shear under different drainage conditions. A strain rate of 0.833 %/min was chosen for all tests based on preliminary testing to ensure drainage based on the matric suction measurements in drained conditions, as well as to ensure hydraulic equilibrium when recording pore pressures in fully undrained conditions. As the cyclic shearing was performed in drained conditions, the valve on the hanging column burette was kept open and matric suction was maintained constant while monitoring any outflow of water from the specimen. Some amount of excess pore water pressures will be generated in any cyclic shearing test regardless of the drainage conditions, but to be considered drained the rate of dissipation should be similar to the rate of generation. In undrained conditions, the valves in the top and bottom caps were closed and the pore water and air pressures are expected to change during cyclic straining. Since radial expansion of the specimen is minimized by the wire-reinforced rubber membrane, the volumetric strain ε_v during cyclic shearing is assumed to be due to changes in height. Shear stress required to apply the cyclic strain with constant amplitude was directly measured using the load cell. The applied vertical total stress for all the specimens was 50 kPa, which represents the stress state of a near-surface backfill soil layer. As each initial condition was assessed in both drained and undrained conditions, a total of 6 tests were performed. The initial specimen height h_0, matric suction ψ_0, degree of saturation S_0, gravimetric water content w_0, volumetric water content θ_{w0}, applied cyclic shear strain γ_c and the gravimetric water content w_f for each specimen after shearing are summarized in Table 2.

Typical test results for sand specimens in dry conditions, nearly-saturated conditions, and unsaturated conditions in the funicular regime (an initial matric suction of 6 kPa) in both drained and undrained conditions are presented and discussed to demonstrate the capabilities of the testing setup in characterizing the hydro-mechanical couplings during seismic compression. The initial states for the different specimens are shown in Figure 5(a). The time series of relevant variables during cyclic shearing are presented to demonstrate capabilities of the test apparatus and to better understand the hydro-mechanical coupling during cyclic shearing. Further, the evolution in the secant shear modulus during cyclic shearing was evaluated by using the measured maximum and minimum shear stresses corresponding to the applied maximum and minimum cyclic shear strains, which provides additional insight into the mechanisms of seismic compression for different drainage conditions.

Results for Dry Sand Specimens

Time histories of the monitored variables during cyclic shearing of dry sand in drained and undrained drainage conditions when subjected to a cyclic strain of 1% under an applied vertical stress of 50 kPa are shown in Figure 8. Since specimens were tested in dry condition, there were no pore water pressure measurements in both drainage conditions. In Figure 8(a), the cyclic shear stress required to maintain the constant shear strain amplitude of 1% increased gradually with number of cycles at a moderate rate in both drainage conditions, as the volume of sand specimens contracted during cyclic shearing which led to a denser state. Dry specimen in undrained condition experienced more seismic compression than that in drained condition, shown in Figure 8(b), which was mainly due to the increased pore air pressure of the dry specimen in undrained condition, as shown in Figure 8(c). The increase in pore air pressure for the dry specimen sheared in undrained conditions led to a decrease in net stress, which caused a softening effect when compared with results for the dry specimen tested in drained conditions. This led to greater seismic compression for the specimen sheared in undrained conditions. Despite this softening effect for the specimen sheared in undrained conditions which led to a lower shear modulus overall, an increase in secant shear modulus with cycles of shearing was observed for the dry soils tested in both drainage conditions, as shown in Figure 8(d). This can be attributed to the densification during cyclic shearing for both soils.

Results for Nearly-Saturated Sand Specimens

Although the sand could not be fully saturated in the current setup due to the lack of backpressure, the degree of saturation of the nearly-saturated specimen was found to reach a value as high as 0.94 using the procedures described above. In this condition, some air bubbles were occluded in the sand specimen and the air phase was disconnected. Accordingly, the pore air pressure was not measured for the nearly-saturated specimens in both drainage conditions. The cyclic shear stress measured during application of cyclic shear strains was observed to increase gradually with number of cycles for the tests performed in drained conditions due to volume contraction, while the measured cyclic shear stress decreased rapidly in the first 30 cycles and then stabilized for the subsequent shearing cycles for the tests performed in undrained conditions, as shown in Figure 9(a). The nearly-saturated specimen still experienced a small amount of volume contraction in undrained condition due to the compressibility of the occluded air bubbles, as shown in Figure 9(b). The decrease in cyclic shear stress in the first 30 cycles of undrained cyclic shearing was primarily due to the increase in pore water pressure and a consequent remarkably decreased effective stress in the first 30 cycles observed in Figure 9(c). The pore water pressure increased at a much slower rate after the first 30 cycles, and the densification of the specimen due to cycles of shearing balanced the softening caused by the increase in excess pore water pressure, which led to the stabilized monitored shear stress observed in Figure 9(a). The stabilization after N = 30 at a cyclic shearing amplitude of 1% is likely specific to the sand tested in this study. The changes in secant shear modulus during shearing under both drainage conditions are shown in Figure 9(d). During drained cyclic shearing, the secant shear modulus increased steadily with number of cycles. However, during undrained cyclic shearing the secant shear modulus was observed to drop significantly in the first 30 cycles, corresponding to the decrease in effective stress associated with the increase in pore water pressure in Figure 9(c), after which it stabilized. Despite this large drop in secant shear modulus, the volumetric contraction was relatively small for the nearly-saturated specimen during undrained shearing due to the relatively small air content.

Results for Unsaturated Sand Specimens

The cyclic shearing test results for an unsaturated specimen with an initial matric suction of 6 kPa are shown in Figure 10. A suction of 6 kPa corresponds to the initial degree of saturation of 0.30 based on the drying path SWRC at the relative density of 0.45. The results in Figure 10(a) indicate that the measured cyclic shear stresses during cyclic shearing at a constant strain amplitude were similar for both drainage conditions, although the values for the specimen sheared in drained condition were slightly higher. It is interesting to observe that undrained cyclic shearing led to more seismic compression than drained cyclic shearing for the specific case in this study shown in Figure 10(b). The reasons for this difference in behavior with drainage conditions could be attributed to the changes in pore water and air pressure as well as the secant shear modulus. For the specimen sheared in drained conditions, air and water in the pores could escape freely from the specimen to maintain the constant suction within the specimen during cyclic shearing, so the effect of matric suction could be isolated. The pore water and pore air pressures were observed to be almost constant throughout the test performed in drained condition as shown in Figures 10(c) and 10(d). The pore water pressure increased slightly by approximately 0.5 kPa in the first few cycles which was due to the temporarily different rate in the generation and dissipation of excess pore water pressure in the unsaturated specimen when cyclic shearing started. However, during undrained cyclic shearing the pore water and air pressures increased at different rates from -6.0 to 0.8 kPa and 0.0 to 4.0 kPa, respectively. These changes in pore air and water pressure are similar to those observed in the undrained cyclic triaxial shearing tests performed by Unno et al. (2008) and Oka et al. (2010). It is also interesting to note that the volumetric strains in Figure 10(b) were still observed to be increasing after N = 200, while the pore water and pore air pressures in Figures 10(c) and 10(d) stabilized after a fewer number of cycles at approximately N = 110. For unsaturated soils, volumetric contraction accumulates during cyclic shearing due to rearrangement of particles into the relatively compressible air-filled voids. During drained shearing, water outflow from the specimen was monitored using the Mariotte tube. The water outflow shown in Figure 10(e) can be used along with the volumetric strain in Figure 10(b) to calculate the degree of saturation for the specimen sheared in drained conditions. As there is no water outflow during undrained shearing, the degree of saturation can be calculated directly from the volumetric strain for the specimen sheared in undrained conditions. Similar to the tests on dry specimens, gradual increases in secant shear modulus were observed for the unsaturated specimens sheared in both drainage conditions, as shown in Figure 10(f). The increases in secant shear modulus can be attributed to the observed densification during drained and undrained cyclic shearing shown in Figure 10(b). Although a decrease in secant shear modulus was not observed for the unsaturated specimen sheared in undrained conditions like that observed for the nearly-saturated specimen sheared in undrained conditions, an interesting observation is that the magnitudes of secant shear modulus were lower for the specimen sheared in undrained conditions. The larger seismic compressions for the unsaturated specimens sheared in undrained conditions could be directly attributed to the smaller secant shear moduli values observed in this figure.

Understanding the difference in the secant shear moduli for the unsaturated specimens sheared in drained and undrained conditions shown in Figure 10(f) requires an interpretation of the evolution in mean effective stress during drained and undrained cyclic shearing. The evolution of relevant variables that affect the mean effective stress during drained and undrained cyclic shearing of the unsaturated sand specimens are shown in Figure 11. Although the results in Figures 10(c) and 10(d) indicate that the pore water and pore air pressures both increased during undrained cyclic shearing, the pore water pressure increased at a greater rate than the pore water pressure. Accordingly, the matric suction was observed to decrease from 6.0 kPa to 3.2 kPa during undrained cyclic shearing, as shown in Figure 11(a). Unno et al. (2008) and Okamura and Noguchi (2009) also observed a decrease in matric suction during undrained cyclic shearing of unsaturated soils. The matric suction was relatively constant during drained cyclic shearing. Because the specimen sheared in undrained conditions experienced volumetric contraction without a change in the volume of water, the degree of saturation was found to increase from 0.207 to 0.218 during undrained cyclic shearing, as shown in Figure 11(b). However, only a slight increase in the degree of saturation from 0.207 to 0.208 was observed during drained cyclic shearing. The effective stress calculated from the matric suction and degree of saturation using Equation (1) with $\chi = S_e$ is shown in Figure 11(c). The results in this figure are interesting as the effective stress for the unsaturated specimen sheared in undrained conditions decreases by nearly 2.5 kPa while the effective stress for the unsaturated specimen sheared in drained conditions remained relatively constant. The decrease in mean effective stress during undrained cyclic shearing helps explain the greater decrease in secant modulus during undrained cyclic shearing. This in turn helps explain the greater amount of volumetric contraction observed during undrained cyclic shearing compared to drained cyclic shearing. Overall, the comparison of the results in Figure 11 confirms that drainage conditions can play a key role in the amount of seismic compression observed in unsaturated soils.

Validation of the Test Results

To validate the results from the cyclic shearing tests on unsaturated sands using the developed apparatus and the proposed methodology, the drained and undrained cyclic shearing test results from this study along with those from other studies that investigated seismic compression of sands under various degrees of saturation are plotted together in Figure 12. This figure includes volumetric strains normalized by the volumetric strains corresponding to the dry conditions in each of these studies due to apparent difference, i.e. testing methodology, soil properties, cyclic loading, drainage conditions, etc. in these studies, which include partially-drained centrifuge shaking table tests by Ghayoomi et al. (2011) where the magnitude of cyclic shear strains are unknown, along with drained and partially-drained cyclic simple shearing tests by Le and Ghayoomi (2017) and Whang et al. (2004, 2005) where the magnitude of cyclic shear strain is smaller than that investigated in this study. Detailed information of the aforementioned experiments as well as the soil tested in these studies are summarized in Table 3. Since there was no reported minimum void ratio of the soil tested in Whang et al. (2004, 2005), the initial density was expressed in terms of relative compaction. The data from Le and Ghayoomi (2017) were reported in terms of the initial suction, so the SWRC was used to estimate the corresponding degree of saturation. Although the soil characteristics, initial densities, magnitude of applied or induced cyclic shear strains, number of cycles applied, drainage conditions and testing methodology are different or unknown for each of these studies which introduced deviations of the test results in Figure 12, similar trends are observed in the results from the drained tests. Specifically, the greatest amounts of seismic compression are observed for dry and saturated specimens, and lower amounts are observed for unsaturated conditions in the funicular regime. The trend from the partially drained centrifuge tests on unsaturated sands also follows a similar trend to the results from the drained tests. While the trends from the undrained tests from this study follow similar trends to the drained tests for low degrees of saturation, a difference in behavior is noted for the nearly-saturated specimen. Since back-pressure saturation could not be used to ensure full saturation of the sand specimens, very small volumetric strains were observed for the nearly-saturated specimen due to the small air content in the initial saturation process in the proposed methodology focusing on characterizing unsaturated sands. If the specimen had been fully saturated, no volumetric strain would have been observed during undrained cyclic shearing. Despite the difference in testing conditions, the results shown in Figure 12 indicate that the apparatus and testing methodology show similar trends to other studies in the literature and thus confirm their validity. Needless to say, the strength of the test device and the proposed testing methodology can be verified by separately controlling the drainage conditions for pore water and pore air in unsaturated sand specimens during testing and thus the effective stress in different drainage conditions, which provides an experimental approach to evaluate the effects of effective stress on the seismic compression of unsaturated sands as well as to calibrate the constitutive models in the literature for unsaturated soils. A limitation of the test apparatus in this study is that it can only be used to understand the seismic compression mechanisms in unsaturated sands up to initial suctions of 11 kPa. To characterize the seismic compression of fine soils with this apparatus, additional advancements including the axis translation technique or vapor flow technique to apply higher suction values would be needed. Further, the suction distribution within the specimen is not uniform but will vary with the elevation head above the fritted glass disk, so the results presented in this study are representative of the location of the tensiometer. Other limitations include issues encountered in the wire-reinforced membranes when applying cyclic shear strains greater than 10%, and possible radial deformations of the wire-reinforced membrane when applying higher axial stresses. Nonetheless, large cyclic shear strains and high vertical stresses are not always encountered in the seismic response of near-surface unsaturated soil layers.

CONCLUSION

A new cyclic simple shear device with a suction-saturation control system was developed to characterize the seismic compression of unsaturated sands when subjected to intermediate to large cyclic shear strains. A special specimen housing was developed for the test apparatus to permit independent measurement of pore water and pore air pressure in unsaturated sands. Sand specimens under a nearly-saturated condition, dry condition, and an unsaturated condition in the funicular regime of the SWRC were assessed using the device. The results obtained during tests under a cyclic strain amplitude of 1% confirm the capability of the test apparatus to consistently capture changes in hydro-mechanical state parameters governing the seismic compression of unsaturated sands. The results from dry and nearly-saturated sand specimens during drained and undrained cyclic shearing highlight the roles of net stress, effective stress and compressibility of the pore air on the seismic compression. Liquefaction was found to not be a concern during undrained cyclic shearing of unsaturated sand specimens with an initial degree of saturation in the funicular regime. The unsaturated sand specimen during undrained cyclic shearing were found to show greater seismic compression than the unsaturated sand specimen during drained cyclic shearing. This was attributed to a lower secant shear modulus for the unsaturated specimen sheared in undrained conditions. This lower secant shear modulus occurred due to complex hydro-mechanical coupling during undrained cyclic shearing. Specifically, a decrease in effective stress occurred during undrained cyclic shearing because the pore water and pore air pressures increased differentially during undrained cyclic shearing, leading to a decrease in matric suction, and the volumetric contraction caused an increase in degree of saturation during undrained cyclic shearing. Overall, the new testing apparatus and methodology was demonstrated to have the capabilities to quantify the relevant variables governing seismic compression of unsaturated soils in different drainage conditions. The insight gained from the analysis of the results emphasizes the importance of considering hydro-mechanical coupling in estimating seismic compression of unsaturated soils.

ACKNOWLEDGMENTS

The authors would like to acknowledge partial financial support provided by the Department of Transportation in California (Caltrans) Project 65A0556 and from the University of California San Diego Academic Senate Grant A050757.

REFERENCES

ASTM D6528-17. *Standard Test Method for Consolidated Undrained Direct Simple Shear Testing of Fine Grain Soils*. ASTM International. West Conshohocken, PA.

Bishop, A. W. 1959. “The Principle of Effective Stress.” Teknisk Ukeblad, 106(39): 859-863.

Bishop, A. W. and G. E. Blight. 1963. “Some Aspects of Effective Stress in Saturated and Partly Saturated Soils.” *Géotechnique*, 13(3): 177-197.

Bjerrum, L. and A. Landva. 1966. “Direct Simple-Shear Tests on a Norwegian Quick Clay.” *Geotechnique*, 16(1): 1-20.

Chaney, R.C. 1978. “Saturation Effects on the Cyclic Strengths of Sand.” In Proceedings of Specialty Conference on Earthquake Engineering and Soil Dynamics. ASCE Pasadena, CA. Vol. 1: 342-358.

Cuomo, S., M. Moscariello, and V. Foresta. 2017. “Wetting Tests of Partially Saturated Soils Under Simple Shear Conditions.” *Géotechnique Letters*, 7(2): 197-203.

Craciun, O. and S. C. R. Lo. 2009. “Matric Suction Measurement in Stress Path Cyclic Triaxial Testing of Unbound Granular Base Materials.” *Geotechnical Testing Journal*, 33(1): 33-44.

Dobry, R. and E. Petrakis. 1990. “Micromechanical Model to Predict Sand Densification by Cyclic Straining.” *Journal of Engineering Mechanics*, 116(2): 288-308.

Doroudian, M. and M. Vucetic. 1995. “A Direct Simple Shear Device for Measuring Small-Strain Behavior.” *Geotechnical Testing Journal*, 18(1): 69-85.

Duku, P. M., J. P. Stewart, D. H. Whang, and E. Yee. 2008. “Volumetric Strains of Clean Sands Subject to Cyclic Loads.” *J of Geotech and Geoenv Eng*, 134(8): 1073-1085.

Dong, Y., N. Lu, and J. S. McCartney. 2016. “Unified Model for Small-Strain Shear Modulus of Variably Saturated Soil.” *J of Geotech and Geoenv Eng*, 142(9), 04016039.

Dong, Y., N. Lu, and J. S. McCartney. 2017. “Scaling Shear Modulus from Small to Finite Strain for Unsaturated Soils.” *J of Geotech and Geoenv Eng*, 144(2), 04017110.

Finn, W. L., P. M. Byrne, and G. R. Martin. 1976. “Seismic Response and Liquefaction of Sands.” *J of Geotech and Geoenv Eng*, 102(8): 841-856.

610 Ghayoomi, M., J. S. McCartney, and H. Y. Ko. 2013. "Empirical Methodology to Estimate Seismically Induced Settlement of Partially Saturated Sand." *J of Geotech and Geoenv Eng*, 139(3): 367-376.

613 Hardin, B. O. and V. P. Drnevich. 1972. "Shear Modulus and Damping in Soil: Design Equations and Curves," *Journal of the Soil Mechanics and Foundations Division*, 98(7): 667-692.

615 Hoyos, L. R., E. A. Suescún-Florez, and A. J. Puppala. 2015. "Stiffness of Intermediate Unsaturated Soil from Simultaneous Suction-Controlled Resonant Column and Bender Element Testing." *Engineering Geology*, 188: 10-28.

618 Ishihara, K., F. Tatsuoka, and S. Yasuda. 1975. "Undrained Deformation and Liquefaction of Sand Under Cyclic Stresses." *Soils and Foundations*, 15(1): 29-44.

620 Ishihara, K. and M. Yoshimine. 1992. "Evaluation of Settlements in Sand Deposits Following Liquefaction during Earthquakes." *Soils and Foundations*, 32(1): 173-188.

622 Ishihara, K. 2001. "Recent Studies on Liquefaction Resistance of Sand-Effect of Saturation." In 4th International Conference on Recent Advances in Geotechnical Earthquake Engineering and Soil Dynamics, San Diego: 1-7.

625 Khosravi, A. and J. S. McCartney. 2009. "Impact of Stress State on the Dynamic Shear Moduli of Unsaturated Compacted soils." In Proceedings of 4th Asia-Pacific Conference on Unsaturated Soils. Newcastle: 1-6.

628 Khosravi, A., M. Ghayoomi, J. S. McCartney, and H. Y. Ko. 2010. "Impact of Effective Stress on the Dynamic Shear Modulus of Unsaturated Sand." *GeoFlorida 2010*: 410-419.

630 Kimoto, S., F. Oka, J. Fukutani, T. Yabuki, and K. Nakashima. 2011. "Monotonic and Cyclic Behavior of Unsaturated Sandy Soil Under Drained and Fully Undrained Conditions." *Soils and Foundations,* 51(4): 663-681.

Le, K. N. and M. Ghayoomi. 2017. "Cyclic Direct Simple Shear Test to Measure Strain-Dependent Dynamic Properties of Unsaturated Sand." *Geotechnical Testing Journal*, 40(3): 381-395.

Lu, N. and W.J. Likos. 2004. *Unsaturated Soil Mechanics*. Wiley and Sons. New York.

Lu, N., J. W. Godt, and D. T. Wu. 2010. "A Closed Form Equation for Effective Stress in Unsaturated Soil." *Water Resources Research*, 46(5): 55-65.

Martin, G. R., W. L. Finn, and H. B. Seed. 1975. "Fundamentals of Liquefaction Under Cyclic Loading." *J of Geotech and Geoenv Eng,* 101(5): 423-438.

McCartney, J. S. and J. M. Parks. 2009. "Uncertainty in Predicted Hydraulic Conductivity Functions of Unsaturated Soils." In Proceedings of the 17th International Conference on Soil Mechanics and Geotechnical Engineering. Alexandria, Egypt: 1618-1621.

Mele, L., J. T. Tian, S. Lirer, A. Flora, and J. Koseki. 2019. "Liquefaction Resistance of Unsaturated Sands: Experimental Evidence and Theoretical Interpretation." *Géotechnique*, 69(6): 541-553.

Milatz, M. and J. Grabe. 2015. "A New Simple Shear Apparatus and Testing Method for Unsaturated Sands." *Geotechnical Testing Journal*, 38(1): 9-22.

Okamura, M. and Y. Soga. 2006. "Effects of Pore Fluid Compressibility on Liquefaction Resistance of Partially Saturated Sand." *Soils and Foundations*, 46(5): 695-700.

Okamura, M. and K. Noguchi. 2009. "Liquefaction Resistances of Unsaturated Non-Plastic Silt." *Soils and Foundations*, 49(2): 221-229.

Oka, F., T. Kodaka, H. Suzuki, Y.S. Kim, N. Nishimatsu, and S. Kimoto. 2010. "Experimental Study on the Behavior of Unsaturated Compacted Silt Under Triaxial Compression." *Soils and Foundations*, 50(1): 27-44.

Pasha, A. Y., A. Khoshghalb, and N. Khalili. 2015. "Pitfalls in Interpretation of Gravimetric Water Content-Based Soil-Water Characteristic Curve for Deformable Porous Media." *International Journal of Geomechanics*, 16(6), D4015004.

Rahnenma, A., G. Habibagahi, and A. Ghahramani. 2003. "A New Simple Shear Apparatus for Testing Unsaturated Soils." *Iranian Journal of Science and Technology*, 27(B1): 73-80.

Rong, W. and J. S. McCartney. 2019. "Effect of Suction on the Drained Seismic Compression of Unsaturated Sand." *In E3S Web of Conferences. EDP Sciences,* Vol. 92, 08004.

Rong, W. and J. S. McCartney. 2020a. "Drained Seismic Compression of Unsaturated Sand." *J of Geotech and Geoenv Eng,* 10.1061/(ASCE)GT.1943-5606.0002251

Rong, W. and J. S. McCartney. 2020b. "Undrained Seismic Compression of Unsaturated Sand." *J of Geotech and Geoenv Eng*, 10.1061/(ASCE)GT.1943-5606.0002420

Rong, W. and J. S. McCartney. 2020c. "Seismic Compression of Unsaturated Sand Under Undrained Conditions." In Geo-Congress 2020: Geo-Systems, Sustainability, Geoenvironmental Engineering, and Unsaturated Soil Mechanics. ASCE, Reston, VA: 299-308.

Seed, H. B. and I. M. Idriss. 1971. "Simplified Procedure for Evaluating Soil Liquefaction Potential." *Journal of Soil Mechanics and Foundations Div*., 97(9): 1249-1273.

Stewart, J. P., J. D. Bray, D. J. McMahon, P. M. Smith, and A. L. Kropp. 2001. "Seismic Performance of Hillside Fills." *J of Geotech and Geoenv Eng,* 127(11): 905-919.

Stewart, J. P., P. M. Smith, D. H. Whang, and J. D. Bray. 2004. "Seismic Compression of Two Compacted Earth Fills Shaken by the 1994 Northridge Earthquake." *J of Geotech and Geoenv Eng*, 130(5): 461-476.

677 Sorbino, G., G. Migliaro, and V. Foresta. 2011. "Laboratory Investigations on Static Liquefaction Potential of Pyroclastic Soils Involved in Rainfall-Induced Landslides of the Flow-Type." In Proceedings of the 5th International Conference on Unsaturated Soils, London, UK. Vol. 1: 375-380.

681 Tatsuoka, F., T. Iwasaki, S. Yoshida, S. Fukushima, and H. Sudo. 1979. "Shear Modulus and Damping by Drained Tests on Clean sand Specimens Reconstituted by Various Methods." *Soils and Foundations*, 19(1): 39-54.

684 Tsukamoto, Y., K. Ishihara, H. Nakazawa, K. Kamada, and Y. Huang. 2002. "Resistance of Partly Saturated Sand to Liquefaction with Reference to Longitudinal and Shear Wave Velocities." *Soils and Foundations*, 42(6): 93-104.

687 Unno, T., M. Kazama, R. Uzuoka, and N. Sento. 2008. "Liquefaction of Unsaturated Sand Considering the Pore Air Pressure and Volume Compressibility of the Soil Particle Skeleton." *Soils and Foundations*, 48(1): 87-99.

690 van Genuchten, M. T. 1980. "A Closed-Form Equation for Predicting the Hydraulic Conductivity of Unsaturated Soils." *Soil Science Society of America Journal*, 44(5): 892-898.

692 Vucetic, M., G. Lanzo, and M. Doroudian. 1998. "Damping at Small Strains in Cyclic Simple Shear Test." *J of Geotech and Geoenv Eng*, 124(7): 585-594.

694 Whang, D., M. F. Riemer, J. D. Bray, J. P. Stewart, and P. M. Smith. 2000. "Characterization of Seismic Compression of Some Compacted Fills." In Advances in Unsaturated Geotechnics: 180-194.

697 Whang, D. H., J. P. Stewart, and J. D. Bray. 2004. "Effect of Compaction Conditions on the Seismic Compression of Compacted Hill Soils." *Geotechnical Testing Journal*, 27(4): 1-9.

Whang, D. H., M. S. Moyneur, P. Duku, and J. P. Stewart. 2005. "Seismic Compression Behavior of Non-Plastic Silty Sands." In Advanced Experimental Unsaturated Soil Mechanics: Proceedings of the International Symposium on Advanced Experimental Unsaturated Soil Mechanics. Eds. A. Tarantino, E. Romero, Y. J. Cui. CRC Press, Boca Raton: 257-263.

Yee, E., J. P. Stewart, and K. Tokimatsu. 2011. *Nonlinear Site Response and Seismic Compression at Vertical Array Strongly Shaken by 2007 Niigata-ken Chuetsu-oki Earthquake*. Report PEER 2011/107. Pacific Earthquake Engineering Research Center. Berkeley, USA.

Yoshimi, Y., K. Tanaka, and K. Tokimatsu. 1989. "Liquefaction Resistance of a Partially Saturated Sand." *Soils and Foundations*, 29(3): 157-162.

Zheng, Y., A. C. Sander, W. Rong, P. J. Fox, P. B. Shing, and J. S. McCartney. 2018. "Shaking Table Test of a Half-Scale Geosynthetic-Reinforced Soil Bridge Abutment." *Geotechnical Testing Journal*, 41(1): 171-192.

Zhou, C., and C. W. W. Ng. 2016. "Effects of Temperature and Suction on Plastic Deformation of Unsaturated Silt Under Cyclic Loads." *Journal of Materials in Civil Engineering*, 28(12), 04016170.

TABLE 1: Hydraulic properties of the unsaturated well-graded sand at a relative density of 0.45 (note: same van Genuchten (1980) SWRC parameters for the wetting and drying paths)

Parameter	Value
van Genuchten (1980) SWRC parameter, α_{vG} (kPa^{-1})	0.70
van Genuchten (1980) SWRC parameter, N_{vG}	2.10
Residual volumetric water content, θ_r	0.00
Volumetric water content at zero suction on drying path, $\theta_{0,\ drying}$	0.38
Volumetric water content at zero suction on wetting path, $\theta_{0,\ wetting}$	0.20
Hydraulic conductivity of saturated soil, k_{sat} (m/s)	1.5×10^{-7}

TABLE 2: Initial conditions of the tested sand specimens

SPECIMENS	h_0 (mm)	ψ_0 (kPa)	S_0	w_0	θ_{w0}
A-1 (nearly-saturated, drained)	20.02	0.02	0.94	0.238	0.380
A-2 (nearly-saturated, undrained)	20.04	0.04	0.94	0.236	0.379
B-1 (unsaturated, drained)	19.95	6.01	0.20	0.049	0.078
B-2 (unsaturated, undrained)	20.03	5.97	0.20	0.052	0.079
C-1 (dry, drained)	19.88	100.00	0.00	0.000	0.000
C-2 (dry, undrained)	19.94	100.00	0.00	0.000	0.000

h_0: Initial specimen height; ψ_0: Initial matric suction; S_0: Initial degree of saturation; w_0: Initial gravimetric water content; θ_{w0}: Initial volumetric water content;

TABLE 3: Details of seismic compression studies from the literature used for comparison with the results from the new device and methodology

	Type of Testing	Soil Description	Initial Density	Initial Degrees of Saturation Studied	Applied Vertical Stress (kPa)	Cyclic Shear Strain Amplitude	Loading Frequency (Hz)	Drainage Conditions	Number of Cycles
Whang et al. (2004)	Strain-controlled Cyclic Simple Shear Test	As-compacted Low-plastic Silty Fines	Relative Compaction, RC = 84%, 88%, 92%	0.62, 0.75, 0.87	101.3	0.1%, 0.4%, 1.0%	1	Partially Drained	15
Whang et al. (2005)	Strain-controlled Cyclic Simple Shear Test	Non-plastic Silty Sand	Relative Compaction, RC = 87%, 92%, 95%	0, 0.30, 0.60	101.3	0.1% - 1%	1	Partially Drained	15
Ghayoomi et al. (2011)	Centrifuge Shake Table Test	F-75 Ottawa Sand	Relative Density, D_r = 45%	0, 0.16, 0.28, 0.50	0	-	40 in model scale, 1 in prototype scale	Partially Drained	15
Le and Ghayoomi (2017)	Strain-controlled Cyclic Simple Shear Test	F-75 Ottawa Sand	Relative Density, D_r = 45%	0, 0.18, 0.19, 0.23, 0.63	50	0.02% - 0.06% (0.05% was selected for comparison)	1	Drained	5

LIST OF FIGURES

FIG. 1. Cyclic simple shear apparatus for unsaturated soils

FIG. 2. Schematic view of the specimen housing with suction-saturation control system (dimensions in mm)

FIG. 3. Details of the components in the specimen housing for unsaturated sands: (a) Wire-reinforced rubber membrane; (b) Top cap with hydrophobic filter; (c) Top view of the bottom platen; (d) Bottom view of the bottom platen

FIG. 4. Particle size distribution curve of the well-graded sand

FIG. 5. Drying- and wetting-path SWRCs of the well-graded sand at D_r = 0.45: (a) SWRCs fitted to the experimental data along with lines delineating regions of water retention; (b) Drying path SWRC showing the approach to determine the air-entry suction (Pasha et al. 2015)

FIG. 6. SSCC of the well-graded sand at D_r = 0.45 plotted in terms of matric suction and degree of saturation

FIG. 7. Applied cyclic shear strains with an amplitude of 1% at a shear strain rate of 0.833%/min: (a) Representative single applied cycle; (b) Example of 200 applied cycles

FIG. 8. Monitored test results for dry sand specimens in drained and undrained conditions: (a) Cyclic shear stress; (b) Volumetric strain; (c) Pore air pressure; (d) Secant shear modulus

FIG. 9. Monitored test results for nearly-saturated sand specimens in drained and undrained conditions: (a) Cyclic shear stress; (b) Volumetric strain; (c) Pore water pressure; (d) Secant shear modulus

FIG. 10. Monitored test results for unsaturated sand specimens with the matric suction of 6 kPa in drained and undrained conditions: (a) Cyclic shear stress; (b) Volumetric strain; (c) Pore water pressure; (d) Pore air pressure; (e) Water outflow data for the drained test with fitted curve; (f) Secant shear modulus

FIG. 11. Evolution of the state parameters for unsaturated sand specimens at an initial matric suction of 6 kPa: (a) Matric suction; (b) Degree of saturation; (c) Mean effective stress

FIG. 12. Comparison of drained and undrained seismic compression results for unsaturated soils having different initial degrees of saturation with results from the literature

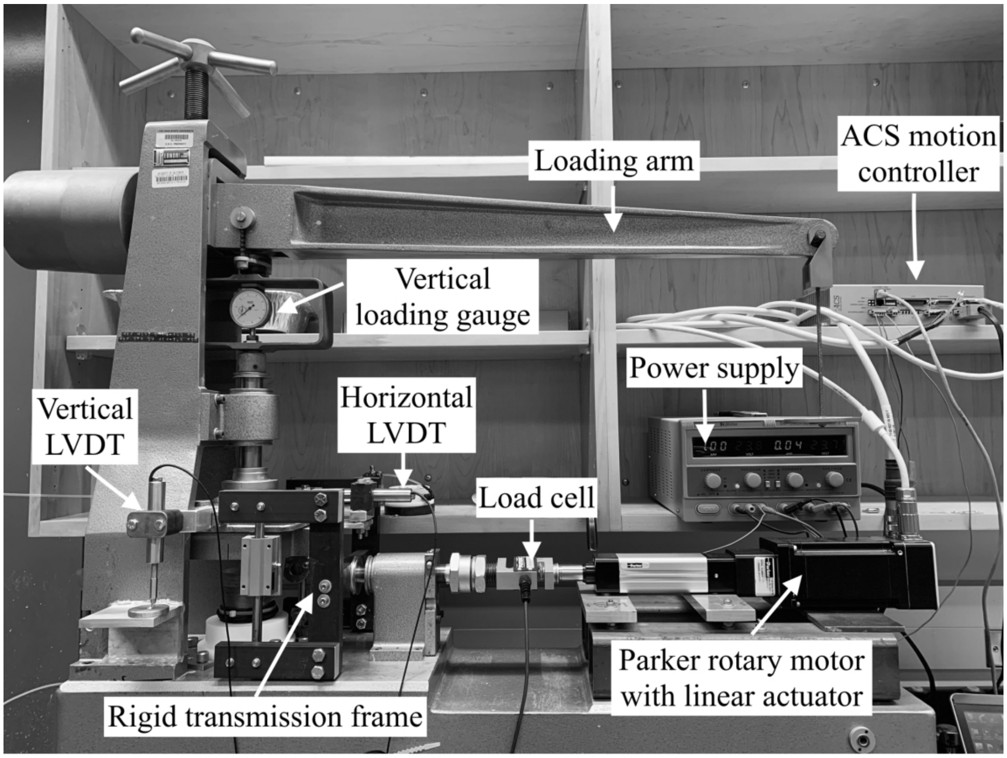

FIG. 1. Cyclic simple shear apparatus for unsaturated soils

88x67mm (600 x 600 DPI)

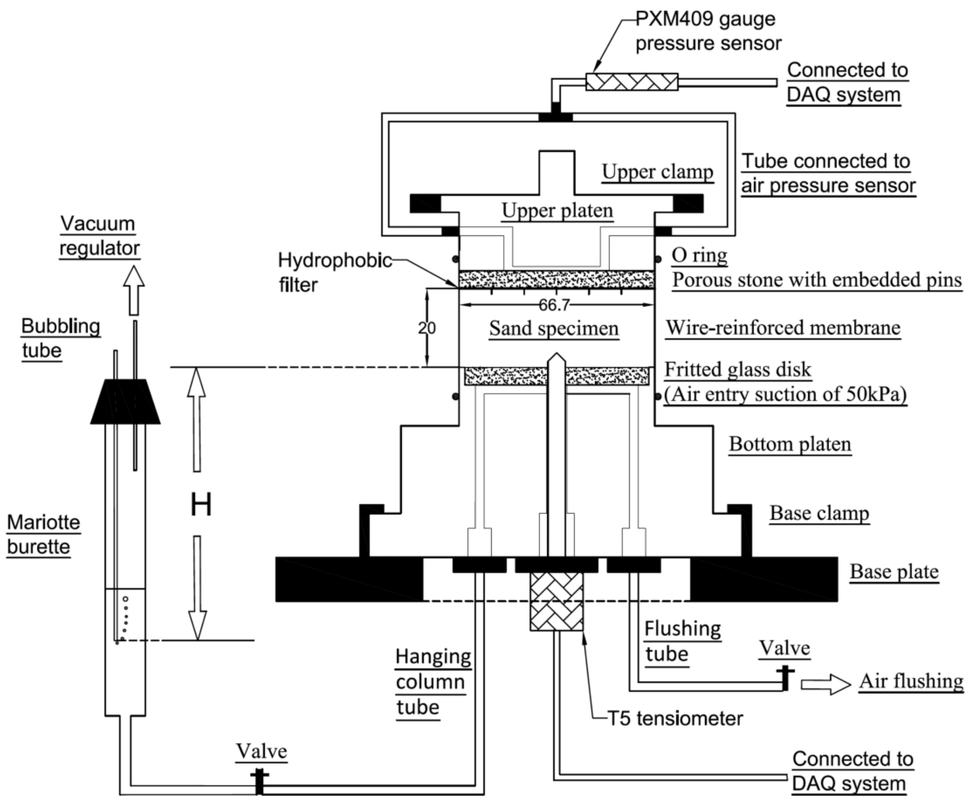

FIG. 2. Schematic view of the specimen housing with suction-saturation control system (dimensions in mm)

177x143mm (600 x 600 DPI)

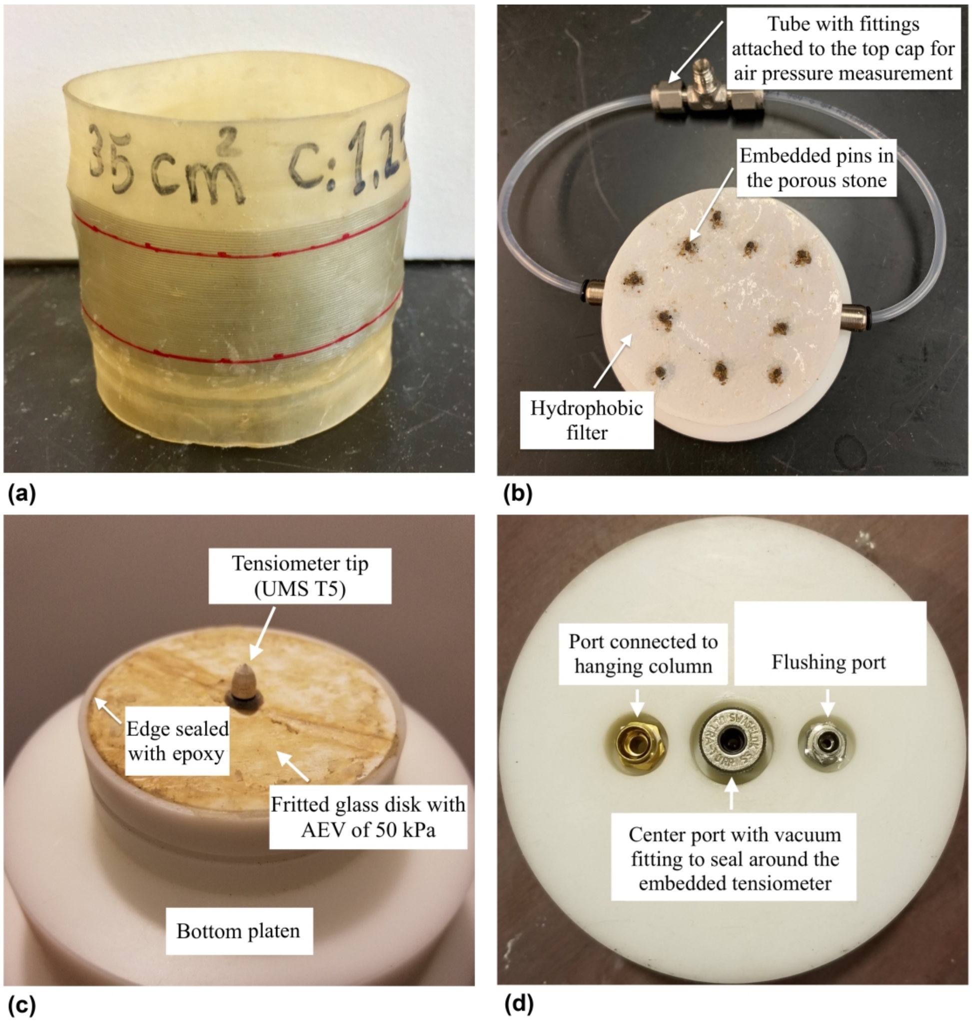

FIG. 3. Details of the components in the specimen housing for unsaturated sands: (a) Wire-reinforced rubber membrane; (b) Top cap with hydrophobic filter; (c) Top view of the bottom platen; (d) Bottom view of the bottom platen

177x181mm (600 x 600 DPI)

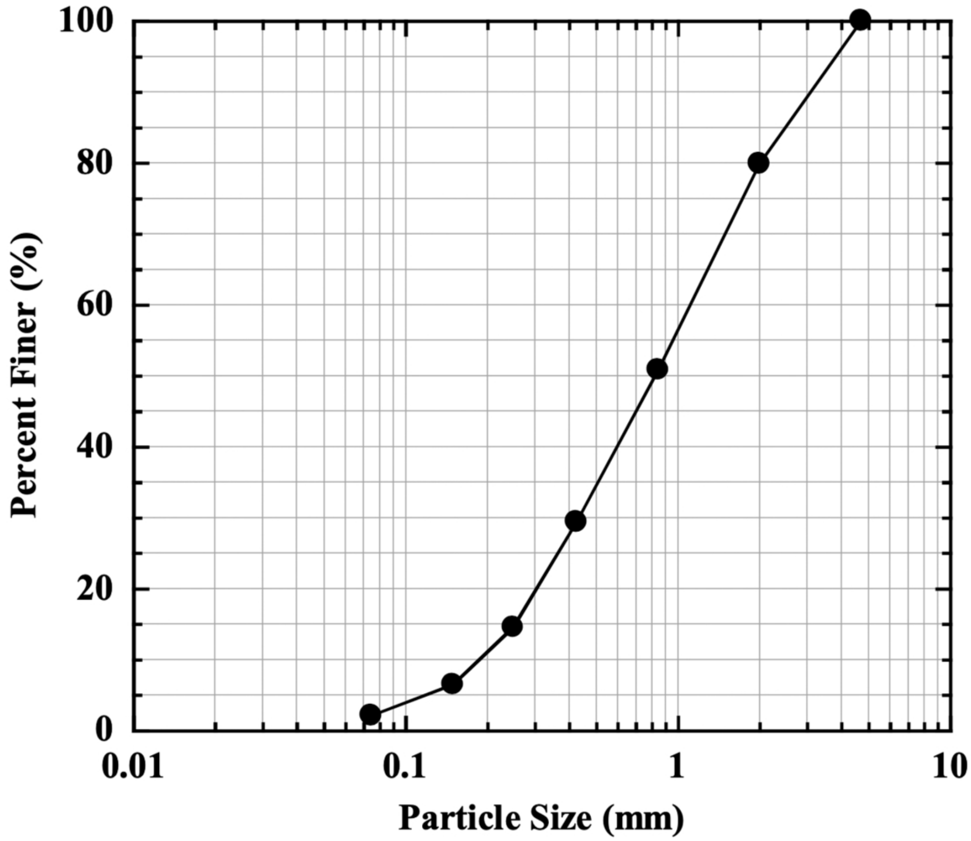

FIG. 4. Particle size distribution curve of the well-graded sand

88x75mm (600 x 600 DPI)

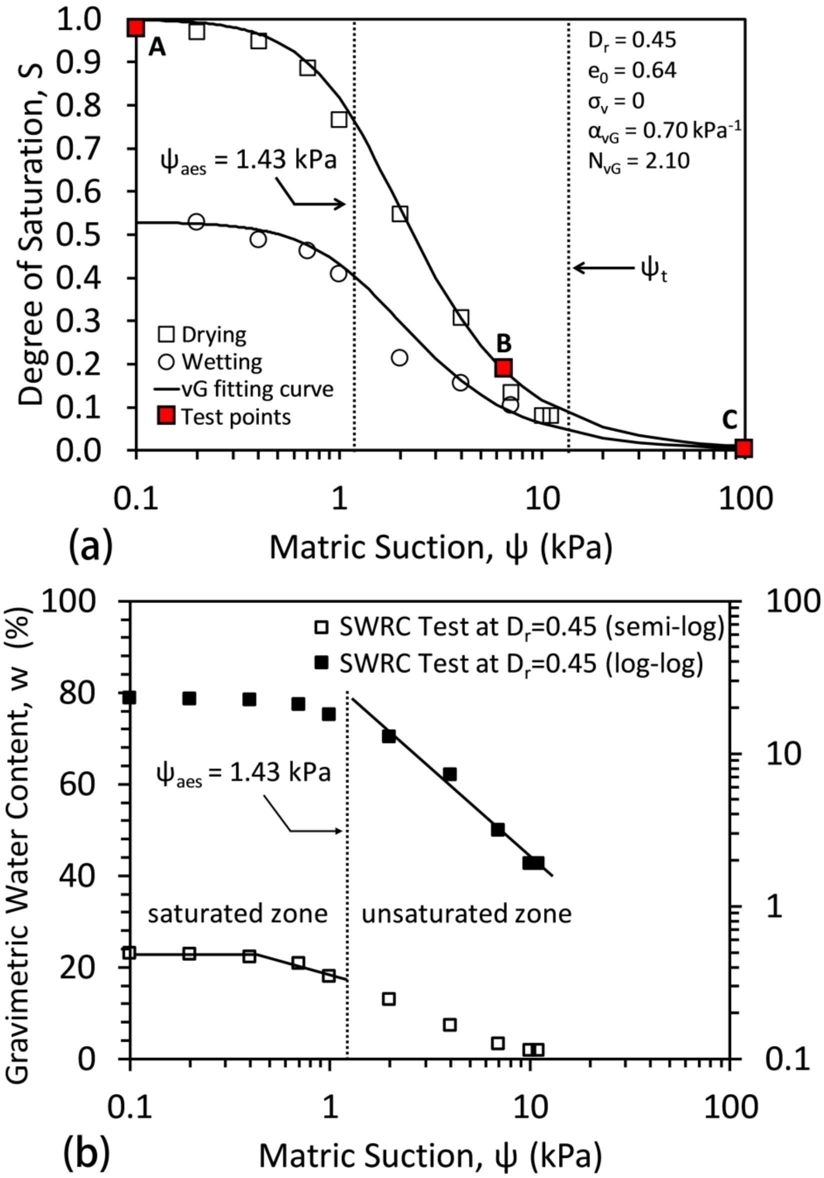

FIG. 5. Drying- and wetting-path SWRCs of the well-graded sand at Dr = 0.45: (a) SWRCs fitted to the experimental data along with lines delineating regions of water retention; (b) Drying path SWRC showing the approach to determine the air-entry suction (Pasha et al. 2015)

88x126mm (600 x 600 DPI)

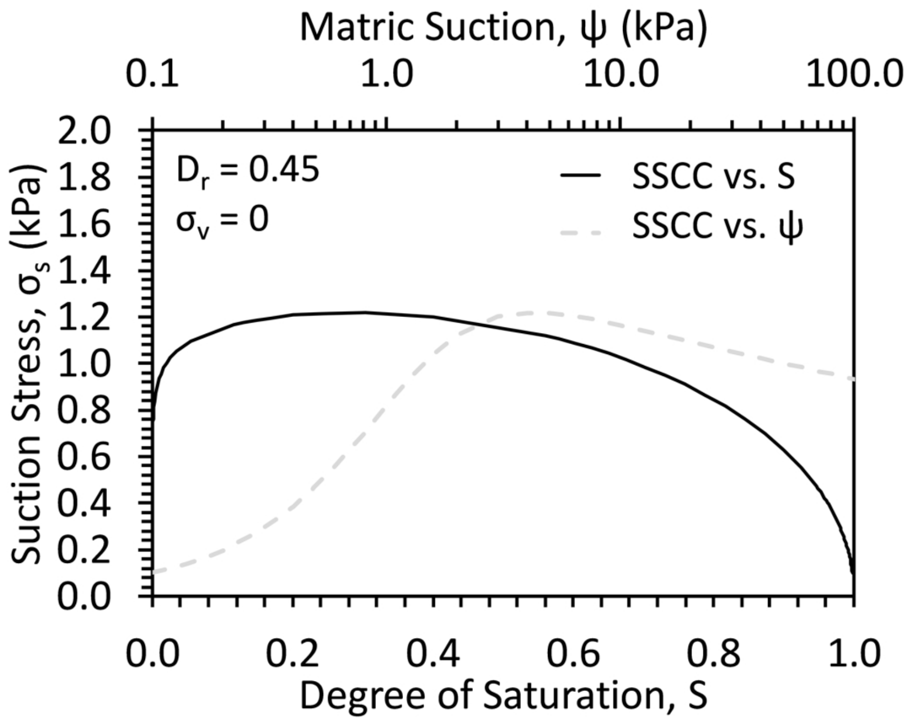

FIG. 6. SSCC of the well-graded sand at Dr = 0.45 plotted in terms of matric suction and degree of saturation

88x65mm (600 x 600 DPI)

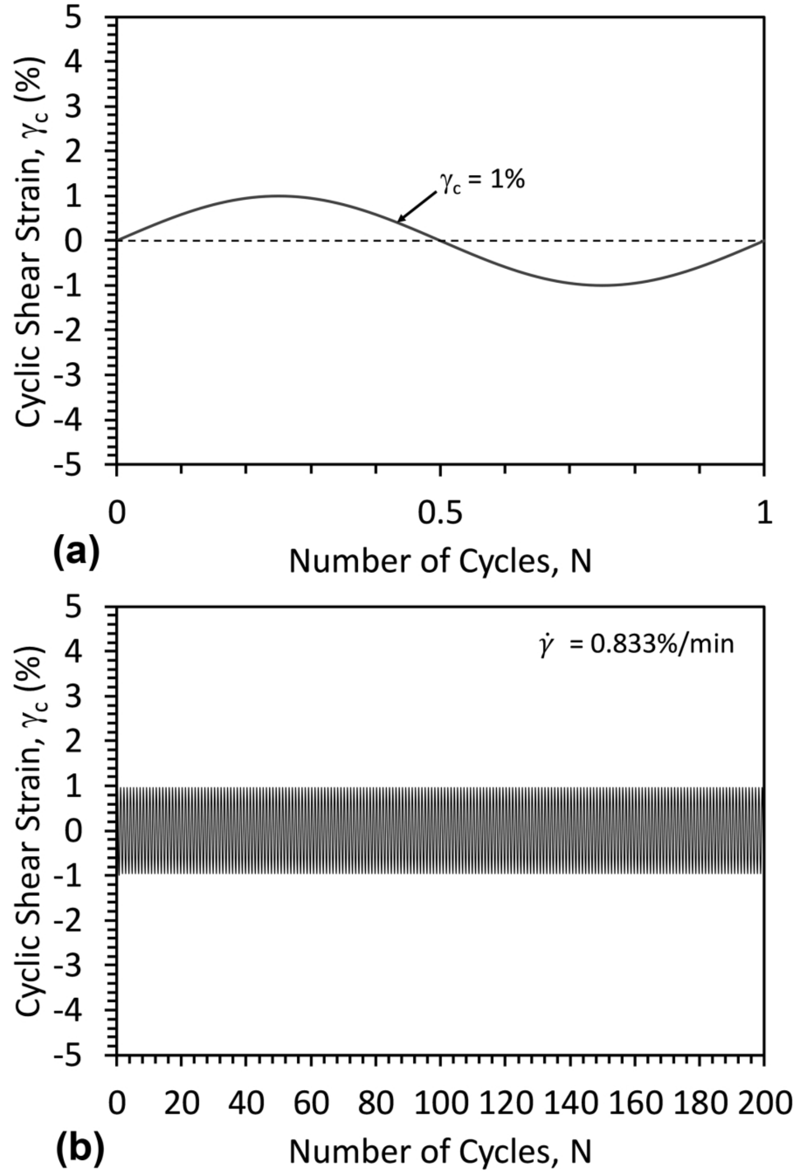

FIG. 7. Applied cyclic shear strains with an amplitude of 1% at a shear strain rate of 0.833%/min: (a) Representative single applied cycle; (b) Example of 200 applied cycles

88x127mm (600 x 600 DPI)

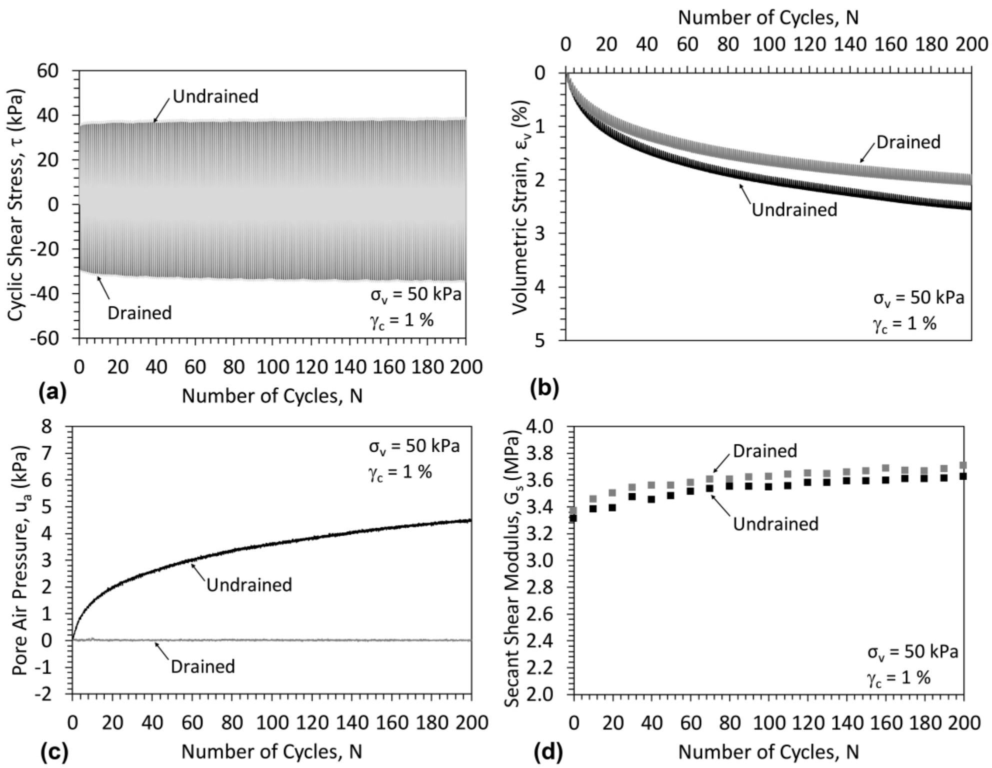

FIG. 8. Monitored test results for dry sand specimens in drained and undrained conditions: (a) Cyclic shear stress; (b) Volumetric strain; (c) Pore air pressure; (d) Secant shear modulus

177x137mm (600 x 600 DPI)

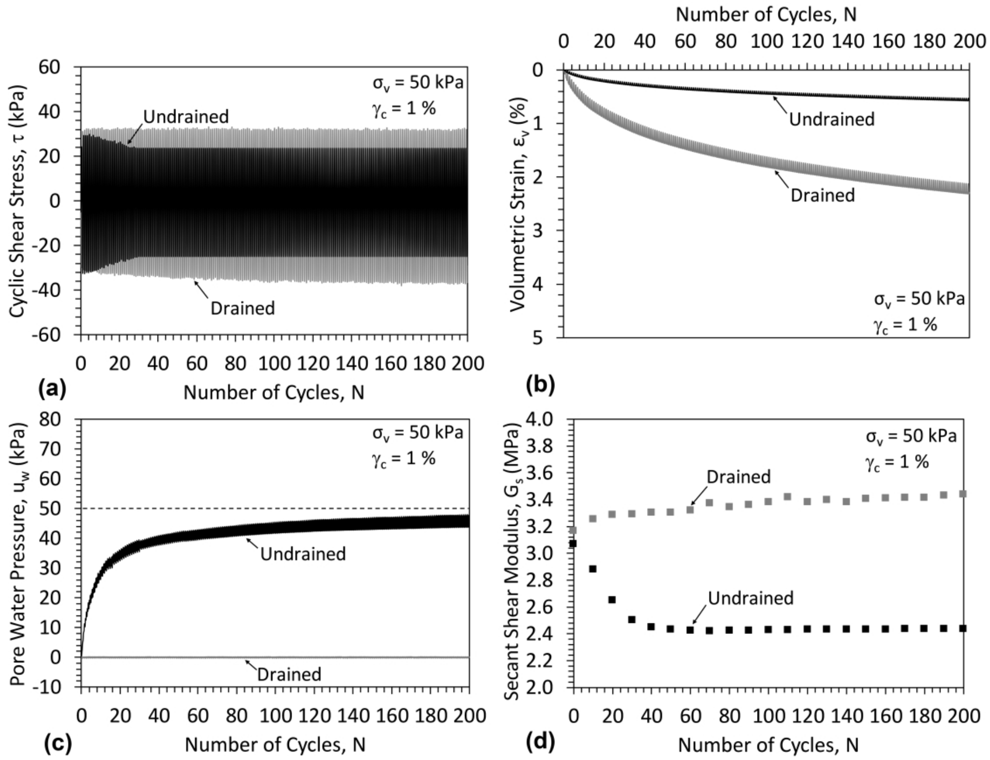

FIG. 9. Monitored test results for nearly-saturated sand specimens in drained and undrained conditions: (a) Cyclic shear stress; (b) Volumetric strain; (c) Pore water pressure; (d) Secant shear modulus

177x136mm (600 x 600 DPI)

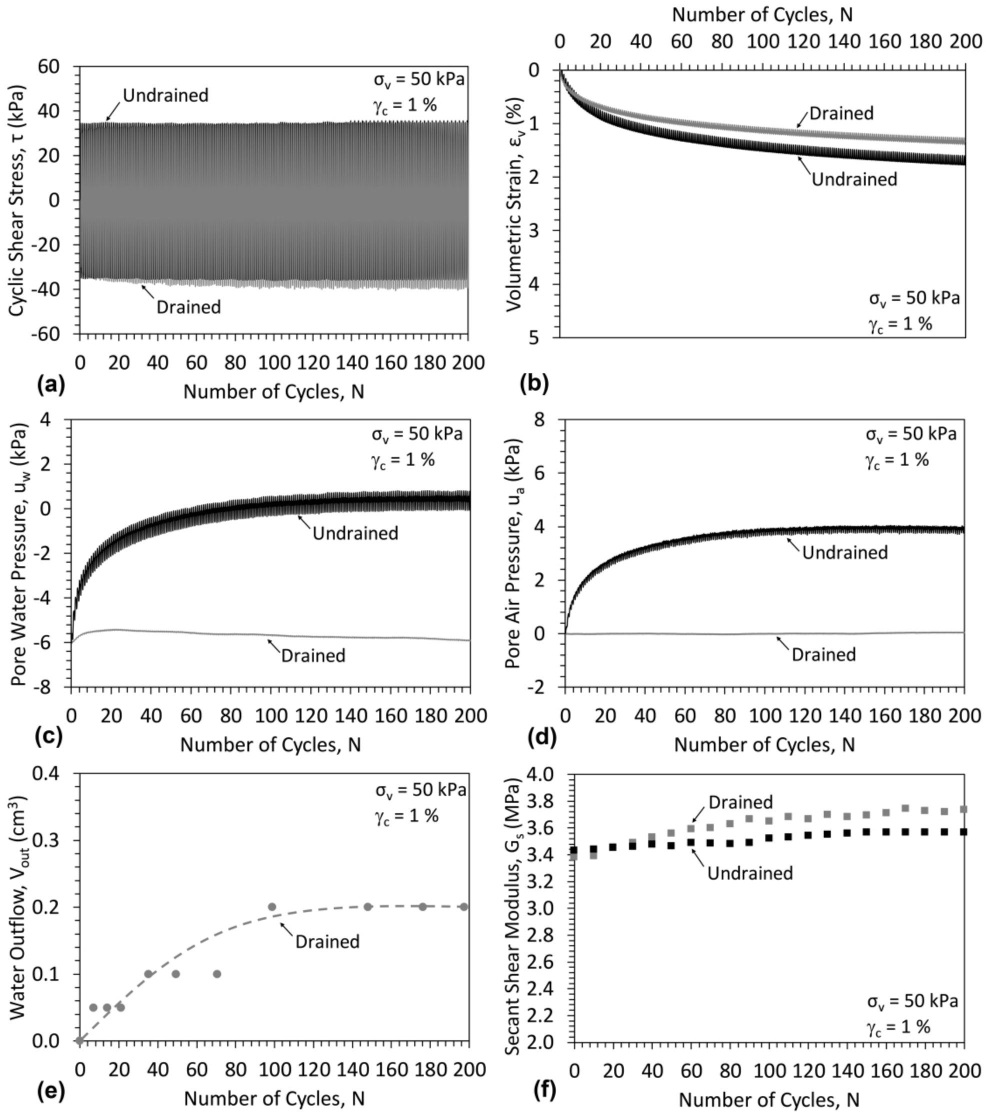

FIG. 10. Monitored test results for unsaturated sand specimens with the matric suction of 6 kPa in drained and undrained conditions: (a) Cyclic shear stress; (b) Volumetric strain; (c) Pore water pressure; (d) Pore air pressure; (e) Water outflow data for the drained test with fitted curve; (f) Secant shear modulus

177x198mm (600 x 600 DPI)

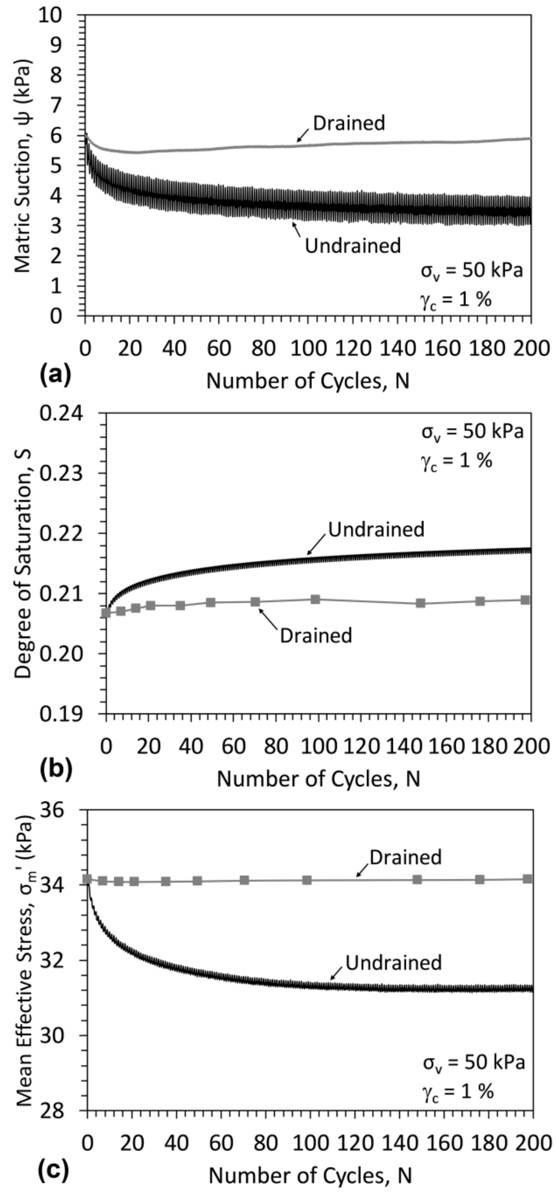

FIG. 11. Evolution of the state parameters for unsaturated sand specimens at an initial matric suction of 6 kPa: (a) Matric suction; (b) Degree of saturation; (c) Mean effective stress

88x189mm (600 x 600 DPI)

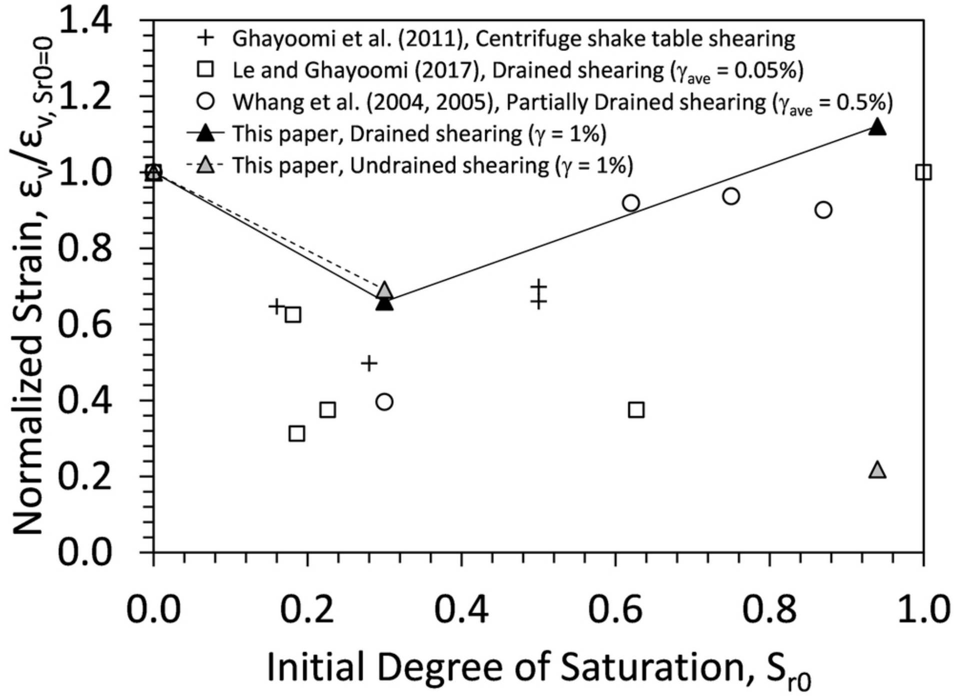

Fig. 12. Comparison of drained and undrained seismic compression results for unsaturated soils having different initial degrees of saturation with results from the literature

88x64mm (300 x 300 DPI)